Materials Science and Engineering C 76 (2017) 727–734

Contents lists available at ScienceDirect

Materials Science and Engineering C

journal homepage: www.elsevier.com/locate/msec

Exploiting biosynthetic gold nanoparticles for improving the aqueous solubility of metal-free phthalocyanine as biocompatible PDT agent

Shaimaa M.I. Alexeree [a], Mahmoud A. Sliem [a], Ragaa M. EL-Balshy [b], Rehab M. Amin [a], M.A. Harith [a,*]

[a] National Institute of Laser Enhanced Science, Cairo University, Egypt
[b] Department of Zoology, Faculty of Science, Benha University, Egypt

ARTICLE INFO

Article history:
Received 10 December 2016
Received in revised form 15 March 2017
Accepted 17 March 2017
Available online 18 March 2017

Keywords:
Biosynthesis
Gold nanoparticles
Metal-free phthalocyanine
Pc-Au nanoconjugates

ABSTRACT

Increasing the limit of dispersion of metal-free phthalocyanine (H_2Pc) in an aqueous medium using biosynthetic gold nanoparticles for photodynamic therapy (PDT) is investigated. Gold nanoparticles (Au NPs) are biosynthesized in one step using Potatoes (*Solanum tuberosum*) extract and are characterized by UV/VIS spectrophotometry, Fourier transformer infrared spectroscopy (FTIR), and transmission electron microscopy (TEM). The metal-free phthalocyanine is conjugated to the surface of the gold nanoparticles in a side to side regime through the secondary amine groups of H_2Pc. The clear violet solution of phthalocyanine-gold (Pc-Au) nanoconjugates is investigated by UV–VIS, FTIR and TEM techniques. Disappearance of the absorption band of the secondary amine in the Pc-Au nanoconjugates compared to that of the parent H_2Pc, and detection of the absorption band of H_2Pc in the aqueous medium confirmed the dispersion of H_2Pc and consequently the loading of H_2Pc on the surface of Au NPs. The cytotoxic effect of biosynthetic gold nanoparticles and Pc-Au nanoconjugates compared to chemically synthesized gold nanoparticles on buffalo epithelial cells has been studied in vitro. Interestingly, the results showed that the biosynthetic Au NPs as well as Pc-Au nanoconjugates have no effect on buffalo epithelial cells viability, which indicating their biocompatibility contrary to the chemically synthesized Au NPs. This work will open the door, for the first time, for using H_2Pc suspended in water for PDT and other phototherapeutic applications.

1. Introduction

Phthalocyanines (Pc) are versatile molecules normally used as photosensitizers. These molecules have strong absorption at short and long wavelength ends of the visible spectrum and are thus well suited for optical applications [1]. Phthalocyanines compounds have unique properties due to their high molar absorption coefficient ε (ca. 10^5 M^{-1} cm^{-1}) in the red part of the spectrum (600–760 nm), which allows increased tissue penetration of the activating light [2]. In addition, low toxicity of phthalocyanines makes them promising agents for PDT applications. Most studies have used phthalocyanine derivatives as hydrophilic photosensitizers. For instance, zinc phthalocyanine (ZnPc), aluminum phthalocyanine (AlPc), silicon phthalocyanine dichloride ($SiPcCl_2$) and copper phthalocyanine (CuPc) have been examined [3].

On the other hand, there are many photosensitizers of hydrophobic nature, such as mesotetra porphyrin, bacteriochlorophylla, verteporfin, methylene blue, hypericin and metal-free phthalocyanines. In order to overcome the problems associated with solubility of such kind of photosensitizers, they have been encapsulated within water soluble polymers [4]. Thus, it is very interesting to develop a drug delivery system based on utilization of nanocarriers to facilitate the injection of hydrophobic photosensitizers and targeting the irradiated tissue at the absorbance maximum of the dye.

Nanobiotechnology refers to the intersection of nanotechnology with biology that has been playing an important role in the field of medical science, biochemical applications, and bioelectronics [5]. The field of nanotechnology is nowadays undergoing rapid development on many rows; through nanoscale drug carriers such as biosynthetic metal nanoparticles that enabled more efficient and safer delivery of drugs [6]. Recently, scientists explored different approaches for delivering multiple therapeutic agents with drug nanocarrier keeping their unique chemical and physical properties. Gold nanoparticles (Au NPs) have been used successfully for the delivery of the readily available photosensitizers such as titanium oxide, protoporphyrin IX, and phthalocyanine derivatives [7].

Novel program is being investigated to get the better of the present barrier of PDT, including the development of a second generation photosensitizer with improved photochemical and tumor localizing

* Corresponding author at: National Institute of Laser enhanced Science, Cairo University, Giza 12316, Egypt.
E-mail address: mharithm@niles.edu.eg (M.A. Harith).

http://dx.doi.org/10.1016/j.msec.2017.03.129
0928-4931/

properties. A lot of the second generation photosensitizers are hydrophobic, typically exhibit better tumor targeting and virtually PDT success [8]. Hone and others have developed Au NPs as carriers of hydrophobic phthalocyanines modified with special function groups to be easily attached to the surface of the nanocarriers [9]. In order to attach the phthalocyanine molecule to the gold surface, the photosensitizer has been derivatized with a thiol moiety. The thiol extends a direct linkage to the Au NPs surface through self-assembly. In such studies, rather than the photosensitizer being encapsulated within the nanoparticle carrier, the photosensitizer is bound to the surface of the Au NPs via a thiol tether specifically designed [10]. The loading of the thiol-terminated phthalocyanine on the Au NPs surface enables the hydrophobic phthalocyanine to dissolve in polar solvents. Moreover, the hydrophobic character of the photosensitizer is maintained so that the conjugates retain the enhanced tumor targeting and high PDT efficacy. The solubility and the overall size of the phthalocyanine-nanoparticle conjugates are essential features as they enable the delivery and the subsequent internalization of the conjugates by the cells. Additional, singlet oxygen does not need to diffuse out as in case of the polymeric/silica nanoparticle structure for per encapsulated photosensitizers [11].

To the best of our knowledge, there isn't any study about the unmodified metal-free phthalocyanine (H_2Pc) or even the direct link of H_2Pc to the surface of a nanocarrier and formation of nanoconjugation. In an attempt to overcome the present limitations of PDT in terms of a need for a vehicle to deliver the drug to the tumor tissue and reduce the toxicity of the phthalocyanine derivatives, we present the current work about the successful conjugation between Au NPs and the hydrophobic unmodified H_2Pc with subsequent dispersion of H_2Pc in aqueous medium. Owing to the wide range of applications offered by metallic nanostructure in different fields of science and technology, various protocols have been designed for their formation [12]. Different chemical and physical synthesis methods are employed in the production of metal nanoparticles. However, these methods use expensive and toxic reagents as reducing and stabilizing agents, and it is very likely that trace amounts of unreacted reagents remain in the solution. Additionally, many problems are often accomplished with the stability, growth and aggregation of the prepared nanoparticles [13].

Nowadays, there is a growing need to develop an environmentally friendly conditions for the synthesis of nanoparticles without using toxic chemicals in the synthesis protocols to avoid adverse effects in medical applications with controlled size and shape in high yield and high purity [14]. The biosynthesis of nanoparticles has been at the center of attention as a green and benign method in recent years [15]. In biological methods where synthesis is carried out by microorganisms, several types of bacteria, yeast and fungi show high ability to synthesize various metallic nanoparticles. Elucidation of the mechanism of plant-mediated synthesis of metal nanoparticles is a very promising area of research. The biosynthetic methods employing plant extracts have received attention as being simple, eco-friendly and economically viable compared to the microbial systems of high pathogenic hazards [16]. It has been demonstrated that Au NPs can be used as efficient drug delivery both in cancer diagnostics and in cancer therapy, as Au NPs show high stability, good biocompatibility, and high surface area. The functionality of the Au NPs can be further enhanced by assembling photoactive molecules on their surfaces [17].

Recently, with increasing the potential use of Au NPs in the field of biomedical and industrial applications, a great attention has been paid to study their nanotoxicity [18]. Many studies have reported the toxicity of Au NPs in vitro, and in vivo [19]. In vitro studies have shown that Au NPs is cytotoxic at relatively high concentrations depending on physical dimension, surface chemistry, and shape of the Au NPs. In general, nanoparticles (NPs) may be expected to be more toxic than larger particles for many reasons; NPs have a higher alveolar deposition leading to prolonged retention, they can go to the lung and enter the blood or lymphatic circulation and their larger surface to mass ratio should lead to faster dissolution compared to larger bulk sized particles [20].

In the current manuscript, we report on the biosynthesis of gold nanoparticles as well as the conjugation between the biosynthesized Au NPs and the hydrophobic unmodified H_2Pc to avoid any chemical hazards and reduce the toxicity. Moreover, we carry out an in vitro toxicity study using biosynthesis Au NPs of 12 nm size as well as Pc-Au nanoconjugates of 20 nm size.

2. Materials and methods

2.1. Materials

All solutions of reacting materials were prepared in deionized water provided by a Milli-Q water purification system. All the glassware were washed with aqua regia ($HCl:HNO_3 = 3:1$ (v/v)) and then rinsed with deionized water. Chlorauric acid ($HAuCl_4$), sodium borohydride (NaBH4), cetyltrimethylammonium bromide (CTAB), L-ascorbic acid (L-AA), phthalocyanine ($C_{32}H_{18}N_8$), dimethylformamide (DMF), polyvinylpyrrolidone (PVP) and sodium hydroxide (NaOH) have been purchased from (Sigma-Aldrich, St. Louis, Missouri, USA). Fresh potato (*Solanum tuberosum*) was purchased from the local market.

2.2. Chemical synthesis of Au NPs

2.2.1. Preparation of Au NPs capped by CTAB

CTAB-capped Au-NPs were synthesized by seed-mediated method with two-step procedures [21]. Firstly, 5 mL of (2.5×10^{-4} mol/L) HAuCl4 was prepared with freshly prepared (3.0×10^{-3} mol/L) ice-cold NaBH4 in the presence of (7.5×10^{-2} mol/L) CTAB. After mixed vigorously for about 30 s, the mixture rapidly changed into light-brown suspension. This mixture was used as seeds for further synthesis of Au-NPs after 2 h. Secondly, 10 mL growth solution was prepared by the reduction of (2.0×10^{-4} mol/L) HAuCl4 with freshly prepared (6.0×10^{-3} mol/L) L-AA in the presence of (1.6×10^{-3} mol/L) CTAB and gently mixed by inversion, with changing in color from orange to colorless immediately. This has been followed by adding 2 h-aged gold seed solution prepared firstly with subsequent change of the color to red gradually. Finally, the mixture was left undisturbed for 24 h. The produced Au NPs were collected and purified by centrifugation at 3000 rpm for 15 min. The process of centrifugation and re-dispersion was repeated many times.

2.2.2. Preparation of Au NPs capped by PVP

PVP-capped Au-NPs were synthesized by reducing a solution of 10^{-3} M $HAuCl_4$ (100 mL) with 300 mL of vigorously stirred ice-cold 2×10^{-3} M $NaBH_4$ [22]. A solution of 1% PVP (50 mL) was added during the reduction. The mixture was then boiled for ca. 1 h to decompose any excess of $NaBH_4$. The gold nanoparticles prepared were pink and had absorption maximum at 520 nm. The synthesis Au NPs were washed and purified by centrifugation at 13000 rpm for 30 min. The process of centrifugation and re-dispersion was repeated three times.

2.3. Biosynthesis of Au NPs

The biosynthesis of Au NPs was performed in a simple way using potatoes extract. For preparation of potatoes extract, about 20 g of peeled potatoes slices were put in a flask supported with 100 mL of double distilled water for a time and then filtered until have clear solution. Afterwards, the pH of the solution was adjusted to be 10.5. A stock solution of $HAuCl_4$ (10 mM) was prepared by dissolving a carefully weighed quantity of $HAuCl_4$ in d.d. water. 3 ml from 10 mM stock solutions of $HAuCl_4$ was added to the clear solution of the potatoes extract to obtain final concentration of 0.3 mM. Upon stirring at 100 °C and after 10 min, the yellow solution turned pink which indicate the reduction of Au^{3+} and production of Au NPs. The biosynthesized Au NPs were collected and purified from potatoes residue by centrifugation at 3000 rpm for 15 min. The process of centrifugation and re-dispersion was repeated

three times. The chemical composition of the potatoes extract was identified using GC–MS analysis. The biosynthesized Au NPs were characterized by UV/VIS spectrophotometry, Fourier transformer infrared spectroscopy (FTIR), and transmission electron microscopy (TEM).

2.4. Preparation of metal-free phthalocyanine – gold (Pc-Au) nanoconjugates

The loading process of the H_2Pc on Au NPs was performed in very facile way. 5 mL of colloidal gold nanoparticles was transferred to several sterile tubes containing different weights of H_2Pc (0.0003, 0.0005 & 0.001 g). The dispersion of H_2Pc in the presence of Au NPs was achieved by sonication for 15 min. The clear violet color was detected and the loading of H_2Pc on the surface of Au NPs was confirmed by UV–VIS, FTIR and TEM techniques.

2.5. Characterization techniques

2.5.1. GC–MS analysis

Identification of Potatoes extract was performed in a gas chromatograph (Agilent GC-6890N), equipped with an Agilent mass spectrometric detector, with a direct capillary interface and fused silica capillary column PAS-5 ms (30 m × 0.32 mm × 0.25 μm film thickness) (Agilent, Palo Alto, CA, USA). Samples were injected under the following conditions:

Helium was used as a carrier gas at approximately 1.0 mL/min, pulsed splitless mode. The solvent delay was 3 min, and the ionization size was 1.0 μL. The mass spectrometric detector was operated in electron impact ionization mode with an ionizing energy of 70 electron volte (eV) scanning from 50 to 500 (m/z). The ion source temperature was 230 °C. The electron multiplier voltage (EM voltage) was maintained at 1650 V above auto tune. The instrument was manually tuned using perfluorotributyl amine (PFTBA). The GC temperature program was started at 60 °C (2 min) them elevated to 300 °C and rate of 5 °C/min. The injector temperature was set at 280 °C. Using computer searches on a NIST Ver.2.1 MS data library and comparing the spectrum obtained through GC–MS, compounds present in potatoes extract were identified.

2.5.2. UV–Vis spectroscopic analysis

The color change in the reaction mixture (metal ion solution + potatoes extract) was recorded through visual observation from colorless to pink. The formation of NPs was monitored by UV–Vis spectroscopy. For absorption measurements, aliquots (200 μL) of the resulting NPs were transferred to 96-well plates, and absorptions were recorded within scan range of 300:700 nm using UV–visible Power Wave microplate spectrophotometer (BioTech, Vermont, USA).

2.5.3. TEM measurements

TEM micrographs were obtained using a JEOL 200 CX (Akishima, Tokyo, Japan) at 200 kV. A droplet of each sample was placed on a copper grid and allowed to dry before being examined in the transmission electron microscope. The TEM images were analyzed using the Image-Pro Plus and Gatan Digital Micrograph program (Yubinbango103-0027 Nihonbashi, Chuo-ku, Tokyo, Japan).

2.5.4. Zeta potential measurements

The surface charge of Au NPs before and after loading of H_2Pc was determined by measurement of zeta potential. The zeta potential was determined using the Malvern Zetasizer Nano ZS 300 HAS (Malvern Instruments, Malvern, UK) at 25 °C and at a 12° angle based on photon correlation spectroscopy. Analysis time was 60 s and the average zeta potential was determined. The zeta potential of nanoparticulate dispersion was determined as such without dilution [23].

2.5.5. FTIR analysis

The FTIR investigations were carried out with a Scimitar Series FTS 2000 Digilab spectrophotometer (Marlborough, MA, USA) in the range of middle infrared of 4000–400 cm^{-1}. For IR spectroscopy, 0.0007 g sample was pressed with 0.2 g of KBr Uvasol® purchased from Merck, Germany. The number of scans was 16 at a resolution of 4 cm^{-1} in these measurements.

2.5.6. Cell cultures

Buffalo epithelial cells (primary culture source: an ear of Egyptian buffalo cultured in CURP, faculty of agriculture, Cairo university) were used as cell models. Cells were grown under aseptic conditions with complete medium in a 25 cm^3 cell culture flask with humidified atmosphere and 5% CO_2 at 37 °C. Cultured monolayer at 80% confluence subjected to wash with PBS (Sigma-Aldrich, St. Louis, Missouri, USA) then trypsinized by 2 mL trypsin–EDTA solution (Sigma-Aldrich, St. Louis, Missouri, USA), incubate for 2 min. Then lightly tapped the flask to detach the cells, to stop the reaction 4 mL complete culture medium was added. The suspended cells have been counted using hemocytometer and cells viability has been checked by trypan blue (99% viability). The cells were diluted with complete medium to have approximately 10^4 cell/mL, and agitated gently. Then the suspended cells were taken and placed in a sterile reservoir. For experimental purposes, cells were cultured in 96-well plates (200 μL of cell suspension per well). Cells were allowed to join for 24 h before treatment.

2.5.7. Cytotoxicity

The 95-C cells were seeded into 60 wells by 200 μL of the buffalo epithelial cells suspension at a density of 2×10^4 cells per well, the peripherals wells were filled with PBS, the plate is incubated for 24 h. Cytotoxicity of the biosynthetic Au NPs and chemically synthesized Au NPs was tested using concentrations ranging from 5 up to 20 (μg/mL). Additionally, cytotoxicity of Pc-Au nanoconjugates was studied using the same concentrations. These concentrations were prepared by dilution with DMEM media (DMEM; Sigma-Aldrich, St. Louis, Missouri, USA). 200 μL of treated media was dispensed into triplicates for each concentration. 10 wells were filled with media only (as a negative control) and two wells filled with media containing Doxorubicin HCL (3 μg/mL, Sigma-Aldrich, St. Louis, Missouri, USA) as a positive control. After that, the 96 wells plate covered by lid was incubated at 37 °C for 24 h. Cell proliferation was then determined by using the Neutral red uptake assay.

2.5.8. Neutral red uptake assay

After the incubation period, the cultures are examined via an inverted microscope (LEICA DMI3000 B, USA), to record changes in the cells morphology. Mitochondrial dehydrogenase activity is an indication for the metabolic and viability of cells. Neutral red uptake assay was performed as follows: 100 μL of neutral red medium (3-amino-7-dimethylamino-2-methyl-phenazinehydrochloride, Sigma-Aldrich cat. no. N4638, USA) (after centrifugation at 1800 rpm for 10 min. to remove any precipitated dye crystals) was added into each well and incubated again for 3 h at 37 °C. After incubation, the dye containing medium was decanted and each well was rinsed gently for three times with 150 μL PBS solutions to remove the unabsorbed neutral red dye contained in the wells. 150 μL of neutral red distain solution (50% ethanol 96% (Riedel-de-Häen), 49% deionized water, 1% glacial acetic acid, Sigma-Aldrich, USA) is added and incubated for 10 min with shaking. The absorbance of acidified ethanol solution containing extracted neutral red dye was measured at 540 nm using spectrophotometer (BioTek ELX808, USA). All assays were carried out in triplicates. The percentage viability was calculated and dose–response curve was plotted for having the concentration of the test chemical reflecting the half maximum inhibitory concentration (IC50) of the cell proliferation [24].

3. Results and discussion

Gold nanoparticles were successfully biosynthesized by exploiting potatoes extract as reducing and stabilizing agents. The chemical composition of the contents of the potato (*Solanum tuberosum*) extract was investigated by GC/MS analysis (Fig. 1). Several components are pronounced in the GC/MS analysis. Oxime-, methoxy-phenyl 79.58%, caffeic acid 10.38%, cyclotrisiloxane, hexamethyl 3.64%, and benzofuran-6-ol-3-one,2-(4-ethoxycarbonyl) benzylidene 1.82% are dominant species in the potatoes extract. The remaining compounds have lower % peak appearing in minute quantities. A great number of phenolic compounds have been detected in potato extract [25], and in our chromatograms oxime, methoxy-phenyl and caffeic acid were observed. The oxime, methoxy-phenyl has sharp band with very high abundance at about 5.36 min [26]. This compound is characterized by the presence of phenolic functional groups that boarded to a hydroxyl groups (—OH) [27]. Furthermore, the caffeic acid has a sharp band at about 9.107 min. The chemical structure of a caffeic acid is characterized by existence of a carboxyl (—COOH) groups as well as a hydroxyl (—OH group) [28]. This clearly explain the role of the content of the potatoes extract in reducing Au^{+3} by phenolic groups and stabilizing the as-prepared Au NPs by phenolic and carboxylic groups.

Mixing the potatoes extract with 0.01 M $HAuCl_4$ aqueous solutions at controlled pH with gentle heating speeds up the reaction. The complete reduction of gold ions was observed after 15 min which results in a change of the yellow color to the characteristics wine red color of Au NPs. This means the reduction of $[Au\ Cl_4]^-$ to Au (0). Mechanism of reduction of gold ions as well as formation and stabilization of Au NPs can be explained in the light of the presence of phenolic and carboxylic compounds in the potatoes extract. These components act as reducing and stabilizing agent under alkaline condition [29].

The reducing ability of oxime-, methoxy-phenyl and caffeic acid at alkaline pH is due to the ionization of the phenolic group in the acid to phenolate ions, which thereafter reduce the gold ions, by electron transfer, into gold atoms and subsequently gold nanoparticles by growth mechanism. In agreement with previous studies [7], the biosynthesized Au NPs were stabilized by the presence of carboxyl groups (—COOH) of a caffeic acid. From these results, we concluded that the caffeic acid probably act as reducing and capping agent for the biosynthesized Au NPs. It is generally believed that the reaction temperature has a great effect on the rate and shape of particle formation. The rate of formation of the nanoparticles was related to the incubation temperature and increased temperature levels allowed particle growth at a faster rate. The time required for the Au NPs formation significantly decreases by increasing the temperature. Therefore, simultaneous mixing of the gold salt with potatoes extract at pH 10.5 and temperature of 100 °C induces the rapid formation of stable gold nanoparticles as indicated by the appearance of the pink color resulting from surface plasmon resonance (SPR) [14].

The H_2Pc is a true hydrophobic photosensitizer. Fig. 2 depicts the chemical structure of metal free phthalocyanine (H_2Pc). With the assistance of the biosynthesized Au NPs and after sonication for a time, about 0.001 g of H_2Pc suspend in 5 mL of gold nanoparticles solution. Loading of the H_2Pc on the surface of Au NPs resulted in changing the characteristic wine red color of the Au NPs to violet color. The appearance of violet color is related to the conjugation of the H_2Pc with the biosynthesized Au NPs which is confirmed by UV–Vis, TEM and FTIR measurements. Schematic representation of the general concept of the biosynthesis of gold nanoparticles and their direct conjugation with the metal-free phthalocyanine (H_2Pc) is clearly shown in Fig. 3.

The UV–Vis absorption spectrum of the H_2Pc dissolved in organic solvent, dimethylformamide (DMF) at concentration 10^{-4} M is shown in Fig. 4. The conventional absorption bands were observed as B and Q bands at 340 nm, 380 nm, 650 nm and 740 nm [1].

The UV–Vis absorption spectrum of the biosynthesized Au NPs with the characteristic absorption peak at 520 nm is shown in Fig. 5 (**spectrum a**). The symmetric SPR band of the Au NPs indicates the formation of monodispersed spherical Au NPs with uniform size and shape. It is well known that the frequency and width of the surface plasmon depend on the particles size, and shape of the gold nanoparticles as well as on the dielectric constant of the metal itself, the surrounding medium and stabilizing molecules [30]. As shown in Fig. 5 (**spectrum b**), the absorption spectrum depicts the presence of Pc-Au nanoconjugates at the wavelength range from 340–760 nm. The spectrum of Pc-Au nanoconjugates shows that the nanoconjugates exhibit characteristic B and Q bands around 300–520 nm and 600–750 nm, respectively [31]. The bands at 340, 380, 650 and 740 nm are attributed to H_2Pc with broadening in the band ranging from 650 to 740 nm probably related to the replacement of secondary amine with tertiary amine after conjugation of the H_2Pc with Au NPs in the aqueous medium. In other words, The broadening of the absorption spectrum (Q-band absorption) of Pc-Au nanoconjugates is related to a tight packing of the H_2Pc on the surface of Au NPs [32]. The band at 520 nm clearly belongs to the presence of the Au NPs in the conjugates. Comparing the two absorption spectra of H_2Pc in organic and aqueous media clearly confirm the dispersion of H_2Pc in the aqueous medium with the assistance of Au NPs

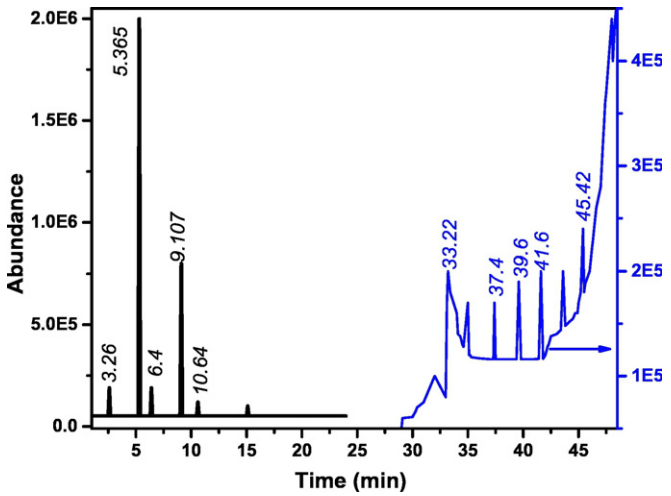

Fig. 1. Chromatogram of the potatoes extracted with characterized peaks.

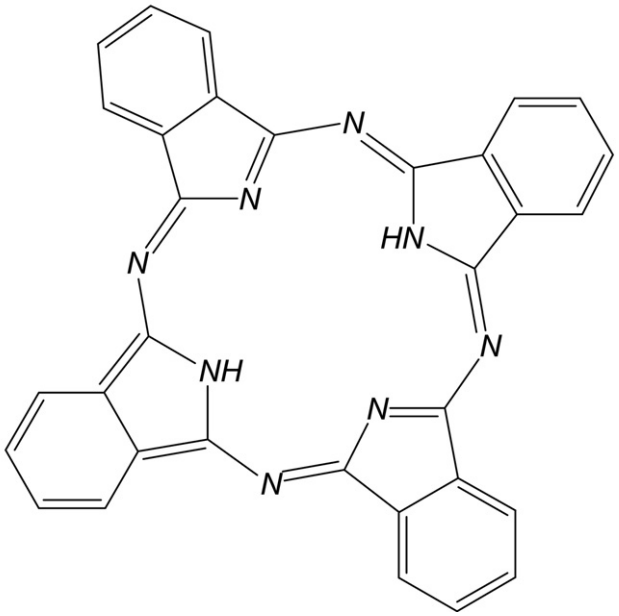

Fig. 2. Chemical structure of metal free phthalocyanine (H_2Pc) (M.W. 514.54 g/mol).

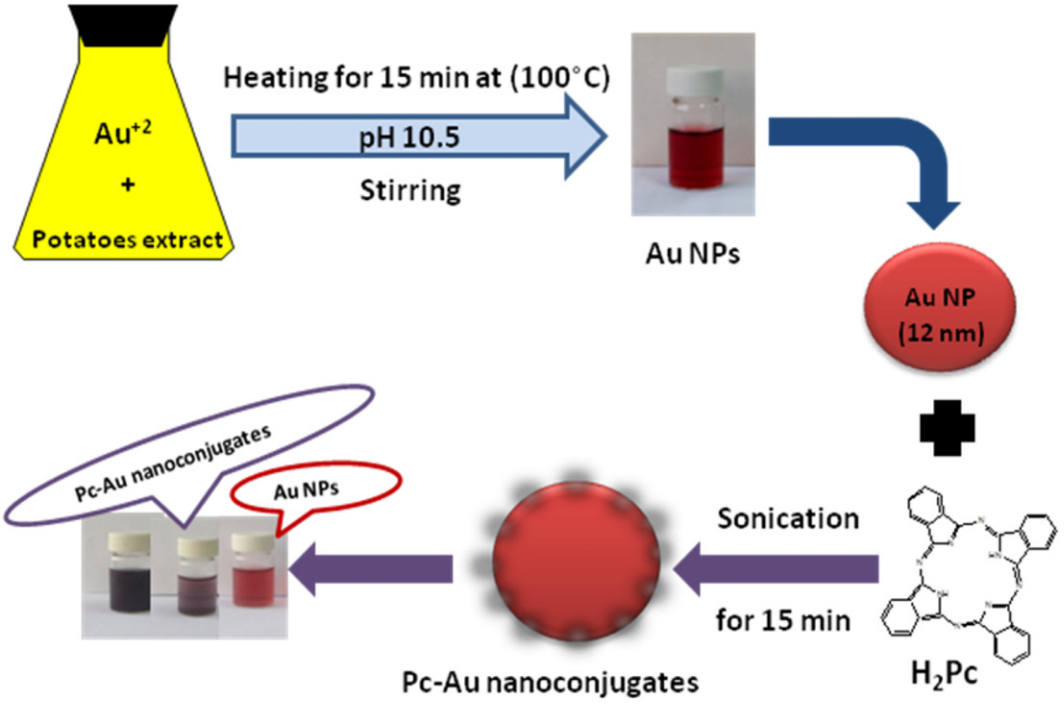

Fig. 3. Schematic representation of the general concept of the biosynthesis of gold nanoparticles from potato (*Solanum tuberosum*) extract and their direct conjugation with the metal-free phthalocyanine (H_2Pc) after sonication for 15 min.

which open the door for hydrophobic photosensitizer like H_2Pc to be utilize in many biological and medical applications. The absorption spectrum of the Pc-Au nanoconjugates indicates the monomeric (non-aggregated) form of phthalocyanine on the surface of Au NPs. This is very important as the aggregated photosensitizer exhibit low PDT efficacy due to deactivation of the excited state energy [33].

Fig. 6a shows the TEM of highly monodispersed spherical shape of the biosynthesized Au NPs with an average size of about 12 nm. The low size distribution of the prepared Au NPs explain clearly the action of the reducing and stabilizing agents present in the potatoes extract. The TEM image of Fig. 6b shows the enlargement of Au NPs from 12 to approximately 20 nm due to loading of H_2Pc on the surface of spherical Au NPs.

The Zeta potential was used to determine the surface charge and the stability of colloidal aqueous dispersions. Usually, a compound with a zeta potential more positive or more negative than 30 mV is considered to be stable. The zeta potential of gold nanoparticles before and after conjugation with H_2Pc is reported as −22.7 and −19 mV, respectively. The Zeta potential measurements revealed that the Au NPs and Pc-Au nanoconjugates are fairly stable in relation to their small size (Fig. 6), and these charge values are enough to keep them stable for long time [34]. The low negative Zeta potential (−19 mV) of the nanoconjugates is in the range known empirically as being safe for membranes and being optimal for cellular uptake [35].

FTIR measurements were carried out in order to get some more insight into the mechanism of the stabilization of the biosynthesized Au NPs, the mechanism of successful loading of H_2Pc on the surface of Au NPs with subsequent dispersion in water and the nature of the function groups of the components of the potatoes extract. Fig. 7 shows the FTIR Spectra of (a) potatoes extract, (b) biosynthesized Au NPs, (c) H_2Pc, and (d) Pc-Au nanoconjugates. FTIR spectrum of Fig. 7a shows the common

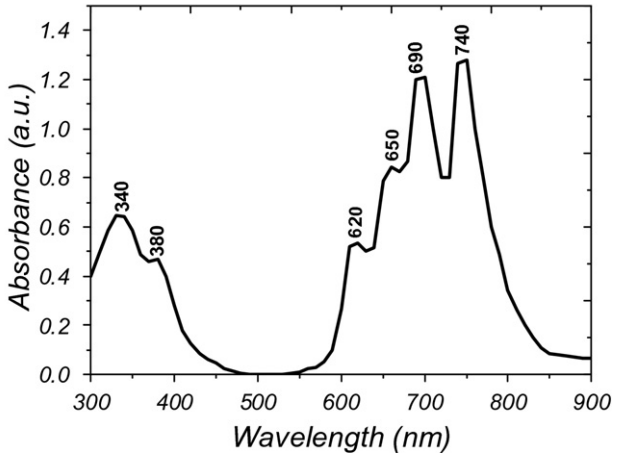

Fig. 4. UV–Vis spectrum of H_2Pc dissolved in (DMF) with assigned characteristic peaks.

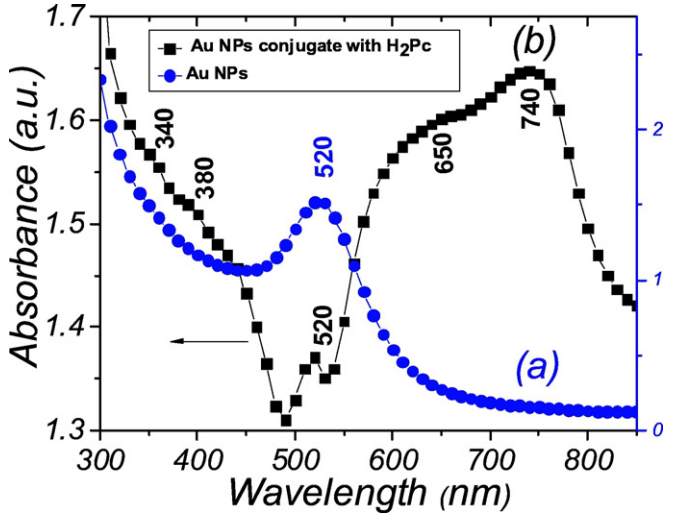

Fig. 5. UV–Vis spectra of (a) biosynthesized Au NPs prepared from potatoes extract with the characteristic peak at about 520 nm and (b) Pc-Au nanoconjugates in the range from 300 to 850 nm.

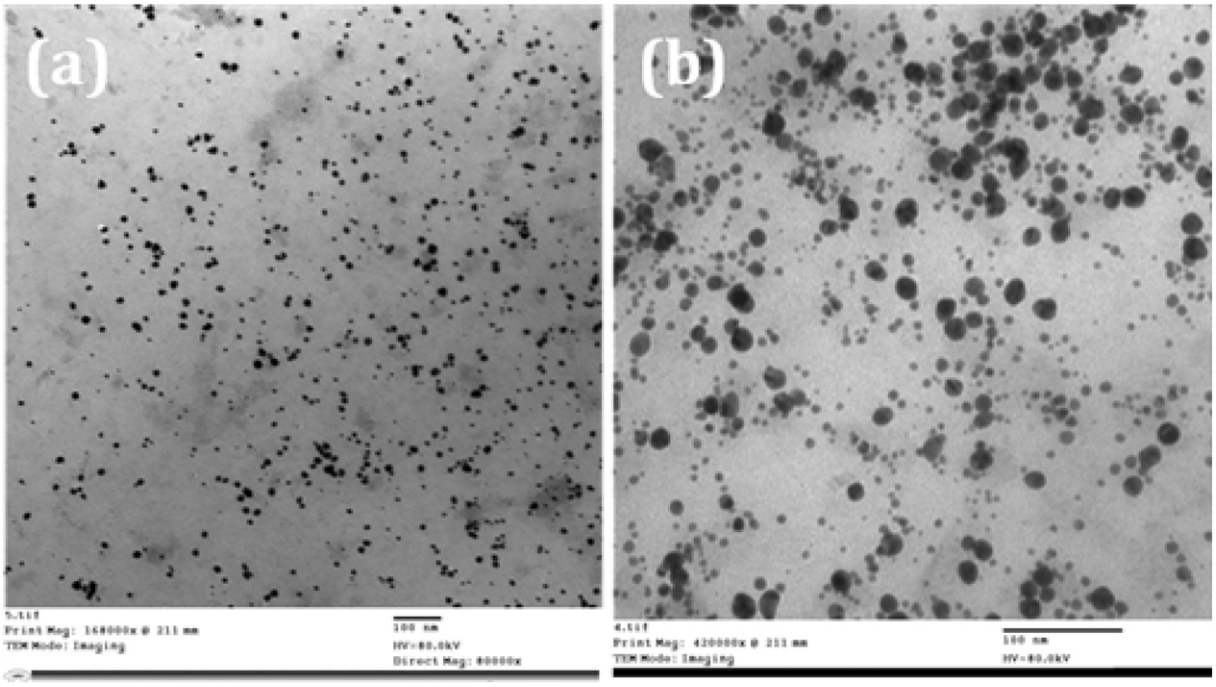

Fig. 6. TEM images of: (a) gold nanoparticles prepared using potatoes extract, spherical in shape with approximate size of 12 nm, and (b) Pc-Au nanoconjugates of spherical shape with increasing size of approximately 20 nm (scale bar = 100 nm).

bands at 543, 612, and 1034 cm^{-1} which ascribed to the C—Br stretching vibration of alkyl halides, alkynes C—H bend group and C—O ether bond of glucose ring of starch, respectively [36]. Additionally, the bands at 1404 and 1610 cm^{-1} are related to the presence of strong bending of —CH_2 and carboxylate groups, respectively [37]. The band at 2926 cm^{-1} in the spectrum is assigned to asymmetric —CH_2 stretch [38]. The FTIR spectrum shows strong absorption at 3400 cm^{-1} which is attributed to OH band stretching mode. The information collected from Fig. 7a is in harmony with GC/MS analysis and confirm the polyphenolic content of the potatoes extract. Among these phonolics are caffeic acid, chlorogenic acid, oxime methoxy-phenyl, ferulic acid, salicylic acid and vanillic acid [39].

Fig. 7b shows the possible interaction sites of gold ions with potatoes extract, which act as reducing agent to synthesize and stabilize Au NPs due to the presence of three main functional groups, including the amino, carboxylic, and phenolic groups. The band at 543 cm^{-1} is ascribed to the C—Br stretching vibration of alkyl halides that appeared more broadening after the reaction with gold ions [40]. The band at 1105 cm^{-1} is attributed to C—N stretching band of the aliphatic amines or to alcohols/phenols [41]. The weak band which appeared at

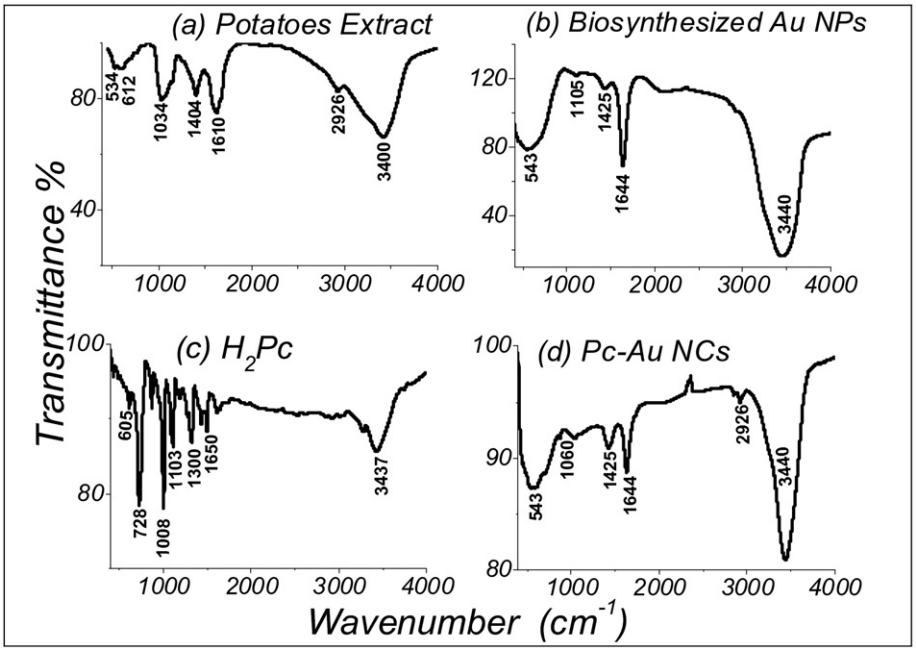

Fig. 7. FTIR absorption spectra with assigned characteristic peaks at certain wavenumbers of (a) potatoes extract, (b) biosynthesized Au NPs, (c) H_2Pc, and (d) Pc-Au nanoconjugates (Pc-Au NCs).

1425 cm^{-1} is ascribed to O═C—CH_2 which represent the interpretation of fingerprint region unique to each compound. The absorption band at 1644 cm^{-1} is assigned to (C═O) amide I band of proteins [42]. The broad band of potatoes extract in the range of 3000–3400 cm^{-1} corresponds to intermolecular hydrogen bond resulting from N—H and O—H stretching vibrations which are characteristic to the functional group of amines and carboxyl found in proteins and phenolic compounds [40,43]. This clearly explains the stabilization of the biosynthesized Au NPs with phenolic and carboxylic groups.

In an attempt to confirm the loading of H_2Pc on the surface of Au NPs through the secondary amines groups of H_2Pc, FTIR measurements were performed again. The FTIR spectra show the characteristic bands of H_2Pc and Pc-Au nanoconjugates (Fig. 7c, d). The most intense infrared active bands of H_2Pc are situated between 400 and 1650 cm^{-1} [44]. The band at 1008 cm^{-1} in the spectrum of H_2Pc originates from N—H (secondary amines) bending vibration [45]. This band is absent in the spectrum of Pc-Au nanoconjugates (Fig. 7d) and replaced by the band at 1060 cm^{-1} which is attributed to tertiary amines as a result of conjugation of H_2Pc to the surface of Au NPs. This conjugation can be achieved through a mechanism of side-to-side interaction between H_2Pc and Au NPs. Vibration band of Au metal is observed in Pc-Au nanoconjugates at 543 cm^{-1} that is not found in the spectrum of H_2Pc [46]. The low metal ligand vibrational frequency could be attributed to the electrostatic repulsion between the outer electron of Au NPs and the electron pair donated by the ligand [47].

From the UV–Vis, TEM, zeta potential, FTIR measurements as well as the complete dispersion of the H_2Pc in the presence of Au NPs with the color change, we can confirm the conjugation between H_2Pc and Au NPs. Accordingly, changing the insoluble H_2Pc into aqueous suspended form makes it possible to use H_2Pc as hydrophobic photosensitizer in many biological and medical applications related to PDT.

In order to investigate the potential use of biosynthetic Au NPs as well as Pc-Au nanoconjugates in various successful applications; it is very essential to study their cytotoxicity. The published reports indicate that buffalo epithelial cells can be used as a model for cytotoxicity of drugs or nanoparticles [48]. The cytotoxicity of Pc-Au nanoconjugates was checked in buffalo epithelial cells using concentrations ranging from 5 up to 20 (μg/mL) for 24 h and showed that there is no effect at low concentration of Pc-Au nanoconjugates (Fig. 8). However, at high concentration, there was a slight inhibition of cell viability. This reflects the very low cytotoxic nature of Pc-Au nanoconjugates [49]. Moreover, the cytotoxicity of biosynthetic Au NPs at doses ranging from 5 up to 20 (μg/mL) for 24 h had a positive effect on the cell viability as it has proliferative effect (Fig. 8). On the other hand, the cytotoxic effect of the Au NPs prepared by chemical methods (CTAB and PVP) was checked in buffalo epithelial cells at the same concentration and showed very high cytotoxicity on cell viability (Fig. 8) [50]. The high cytotoxic effect of Au capped by CTAB and those capped by PVP is attributed to the chemical composition of the surface ligands of chemically synthesized Au NPs. The data is presented in percentages of cell survival in relation to the negative control.

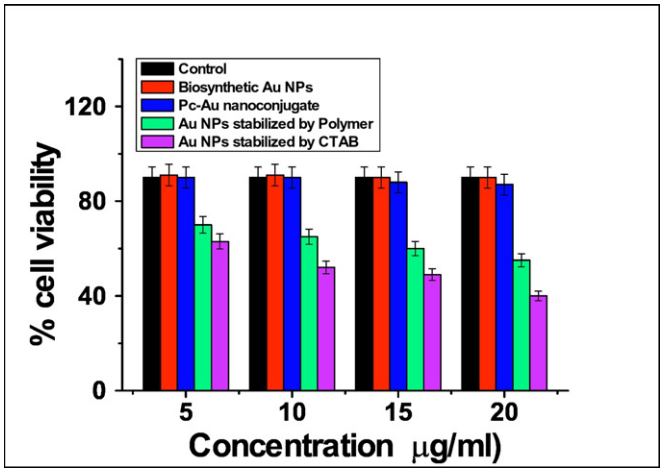

Fig. 8. Cell viability assay of buffalo epithelial cells in case of control, biosynthetic Au NPs, Pc-Au nanoconjugates, Au NPs capped by polymer (PVP), and Au NPs capped by CTAB, for 24 h. Cell viability was determined by a neutral red uptake assay.

4. Conclusion

The present work presents for the first time a new approach for a new generation of hydrophobic photosynthesizers to be utilized in aqueous media. We have developed a fast, eco-friendly, cost effective and convenient method for the synthesis of gold nanoparticles using potatoes extract. The process is a one step synthesis in a short time compared to traditional methods. Nanoparticles synthesized by this method were controlled in size, monodispersed spherically shaped and stable for several months. This green biosynthesis method would be a better alternative to the existing physical and chemical methods and present nanocarriers (Au NPs) free from reducing and stabilizing chemicals of high toxicity. The presented approach provides the conjugation between the hydrophobic photosynthesizer, like H_2Pc, and promising biocompatible nanocarrier, like Au NPs, with subsequent suspension of H_2Pc in water. The biosynthetic Au NPs as well as Pc-Au nanoconjugates showed high biocompatibility in vitro. The successful formation of Pc-Au nanoconjugates opens the door for the use of the hydrophobic photosynthesizers and drugs in many biological and medical applications. Future work is in progress to investigate the positive effects of Pc-Au nanoconjugates as an important PDT agent for skin cancer treatment.

References

[1] http://connection.ebscohost.com/c/articles/99717713/ (accessed on 20 September 2016).
[2] A. Zielichowska, J. Saczko, A. Garbiec, M. Dubińska-Magiera, J. Rossowska, P. Surowiak, A. Choromańska, M. Daczewska, J. Kulbacka, H. Lage, The photodynamic effect of far-red range phthalocyanines (AlPc and Pc green) supported by electropermeabilization in human gastric adenocarcinoma cells of sensitive and resistant type, Biomed. Pharmacother. 69 (2015) 145–152.
[3] L. Sobotta, M. Wierzchowski, M. Mierzwicki, Z. Gdaniec, J. Mielcarek, L. Persoons, T. Goslinski, J. Balazarini, Photochemical studies and nanomolar photodynamic activities of phthalocyanines functionalized with 1,4,7-trioxanonyl moieties at their non-peripheral positions, J. Inorg. Biochem. 155 (2016) 76–81.
[4] A.B. Ormond, H.S. Freeman, Dye sensitizers for photodynamic therapy, Materials 6 (3) (2013) 817–840.
[5] V. Kumar, S.K. Yadav, Plant-mediated synthesis of silver and gold nanoparticles and their applications, J. Chem. Technol. Biotechnol. 84 (2) (2009) 151–157.
[6] C. Engelbrekt, K.H. Sørensen, J. Zhang, A.C. Welinder, P.S. Jensen, J. Ulstrup, Green synthesis of gold nanoparticles with starch–glucose and application in bioelectrochemistry, J. Mater. Chem. 19 (42) (2009) 7839.
[7] S. Sortino, A. Mazzaglia, L. Monsù Scolaro, F. Marino Merlo, V. Valveri, M.T. Sciortino, Nanoparticles of cationic amphiphilic cyclodextrins entangling anionic porphyrins as carrier-sensitizer system in photodynamic cancer therapy, Biomaterials 27 (23) (2006) 4256–4265.
[8] I. Maliszewska, Microbial mediated synthesis of gold nanoparticles: preparation, characterization and cytotoxicity studies, Dig. J. Nano. Biostruct. 8 (2013) 1123–1131.
[9] N.F. Gamaleia, E.D. Shishko, G.A. Dolinsky, A.B. Shcherbakov, A.V. Usatenko, V.V. Kholin, Photodynamic activity of hematoporphyrin conjugates with gold nanoparticles: experiments in vitro, Exp. Oncol. 32 (1) (2010) 44–47.
[10] D.C. Hone, P.I. Walker, R. Evans-Gowing, S. FitzGerald, A. Beeby, I. Chambrier, M.J. Cook, D.A. Russell, Generation of cytotoxic singlet oxygen via phthalocyanine-stabilized gold nanoparticles: a potential delivery vehicle for photodynamic therapy, Langmuir 18 (8) (2002) 2985–2987.
[11] T.P. Mthethwa, S. Tuncel, M. Durmuş, T. Nyokong, Photophysical and photochemical properties of a novel thiol terminated low symmetry zinc phthalocyanine complex and its gold nanoparticles conjugate, Dalton Trans. 42 (14) (2013) 4922.
[12] A. Madhusudhan, G. Reddy, M. Venkatesham, G. Veerabhadram, D. Kumar, S. Natarajan, M.Y. Yang, A. Hu, S. Singh, Efficient pH dependent drug delivery to target cancer cells by gold nanoparticles capped with carboxymethyl chitosan, Int. J. Mol. Sci. 15 (5) (2014) 8216–8234.
[13] S.A. Kumar, Y.A. Peter, J.L. Nadeau, Facile biosynthesis, separation and conjugation of gold nanoparticles to doxorubicin, Nanotechnology 19 (49) (2008) 495101.
[14] K.D. Arunachalam, S.K. Annamalai, *Chrysopogon zizanioides* aqueous extract mediated synthesis, characterization of crystalline silver and gold nanoparticles for biomedical applications, Int. J. Nanomedicine 8 (2013) 2375–2384.

[15] T.X. Phuoc, Complete green synthesis of gold nanoparticles using laser ablation in deionized water containing chitosan and starch, J. Mater. Sci. Nanotechnol. 1 (2014) 401.
[16] C. Shi, N. Zhu, Y. Cao, P. Wu, Biosynthesis of gold nanoparticles assisted by the intracellular protein extract of *Pycnoporus sanguineus* and its catalysis in degradation of 4-nitroaniline, Nanoscale Res. Lett. 10 (1) (2015) 147–154.
[17] P.C. Chen, S.C. Mwakwari, A.K. Oyelere, Gold nanoparticles: from nanomedicine to nanosensing, Nanotechnol. Sci. Appl. 1 (2008) 45–65.
[18] N. Khlebtsov, L. Dykman, Biodistribution and toxicity of engineered gold nanoparticles: a review of in vitro and in vivo studies, Chem. Soc. Rev. 40 (2011) 1647–1671.
[19] S.J. Soenen, P. Rivera-Gil, J.M. Montenegro, W.J. Parak, S.C. Smedt, K. Braeckmans, Cellular toxicity of inorganic nanoparticles: common aspects and guidelines for improved nanotoxicity evaluation, Nano Today 6 (5) (2011) 446–465.
[20] N.M. Schaeublin, L.K. Braydich-Stolle, A.M. Schrand, J.M. Miller, J. Hutchison, J.J. Schlager, S.M. Hussain, Surface charge of gold nanoparticles mediates mechanism of toxicity, Nano 3 (2) (2011) 410–420.
[21] Y. Wang, L. Zhan, C.Z. Huang, One-pot preparation of dextran-capped gold nanoparticles at room temperature and colorimetric detection of dihydralazine sulfate in uric samples, Anal. Methods 2 (12) (2010) 1982–1988.
[22] P.C. Lee, D. Meisel, Adsorption and surface-enhanced Raman of dyes on silver and gold sols, J. Phys. Chem. 86 (17) (1982) 3391–3395.
[23] M.A. Dobrovolskaia, A.K. Patri, J. Zheng, J.D. Clogston, N. Ayub, P. Aggarwal, B.W. Neun, J.B. Hall, S.E. McNeil, Interaction of colloidal gold nanoparticles with human blood: effects on particle size and analysis of plasma protein binding profiles, Nanomedicine 5 (2) (2009) 106–117.
[24] G. Repetto, A. del Peso, J.L. Zurita, Neutral red uptake assay for the estimation of cell viability/cytotoxicity, Nat. Protoc. 3 (7) (2008) 1125–1131.
[25] H. Akyol, Y. Riciputi, E. Capanoglu, M.F. Caboni, V. Verardo, Phenolic compounds in the potato and its byproducts: an overview, Int. J. Mol. Sci. 17 (6) (2016) 1422–1441.
[26] S.R. Kanatt, R. Chander, P. Radhakrishna, A. Sharma, Potato peel extract a natural antioxidant for retarding lipid peroxidation in radiation processed lamb meat, J. Agric. Food Chem. 53 (5) (2005) 1499–1504.
[27] R. Ezekiel, N. Singh, S. Sharma, A. Kaur, Beneficial phytochemicals in potato — a review, Food Res. Int. 50 (2) (2013) 487–496.
[28] E. Ngadze, T.A. Coutinho, D. Icishahayo, J.E. Waals, Effect of calcium soil amendments on phenolic compounds and soft rot resistance in potato tubers, Crop. Prot. 62 (2014) 40–45.
[29] Y. Kono, K. Kobayashi, S. Tagawa, K. Adachi, A. Ueda, Y. Sawa, H. Shibata, Antioxidant activity of polyphenolics in diets: rate constants of reactions of chlorogenic acid and caffeic acid with reactive species of oxygen and nitrogen, Biochim. Biophys. Acta 1335 (3) (1997) 335–342.
[30] W. Haiss, N.T.K. Thanh, J. Aveyard, D.G. Fernig, Determination of size and concentration of gold nanoparticles from UV—vis spectra, Anal. Chem. 79 (11) (2007) 4215–4221.
[31] L.A. Muehlmann, M.C. Rodrigues, J.P.F. Longo, M.P. Garcia, K.R. Py-Daniel, A.B. Veloso, P.E. Narciso de Souza, S.W. da Silva, R.B. Azevedo, Aluminium-phthalocyanine chloride nanoemulsions for anticancer photodynamic therapy: development and in vitro activity against monolayers and spheroids of human mammary adenocarcinoma MCF-7 cells, J. Nanobiotechnol. 13 (2015) 36–47.
[32] N. Nombona, E. Antunes, C. Litwinski, T. Nyokong, Synthesis and photophysical studies of phthalocyanine–gold nanoparticle conjugates, Dalton Trans. 40 (44) (2011) 11876–11884.
[33] M.E. Wieder, D.C. Hone, M.J. Cook, M.M. Handsley, J. Gavrilovic, D.A. Russell, Intracellular photodynamic therapy with photosensitizer-nanoparticle conjugates: cancer therapy using a 'Trojan horse', Photochem. Photobiol. Sci. 5 (8) (2006) 727–734.
[34] R. Guillet-Nicolas, A. Popat, J.L. Bridot, G. Monteith, S.Z. Qiao, F. Kleitz, pH-responsive nutraceutical–mesoporous silica nanoconjugates with enhanced colloidal stability, Angew. Chem. Int. Ed. 52 (8) (2013) 2318–2322.
[35] M.A. Rather, R. Sharma, S. Gupta, S. Ferosekhan, V.L. Ramya, S.B. Jadhao, Chitosan-nanoconjugated hormone nanoparticles for sustained surge of gonadotropins and enhanced reproductive output in female fish, PLoS One 8 (2) (2013), e57094.
[36] F. Buazar, M. Bavi, F. Kroushawi, M. Halvani, A. Khaledi-Nasab, S.A. Hossieni, Potato extract as reducing agent and stabiliser in a facile green one-step synthesis of ZnO nanoparticles, J. Exp. Nanosci. 11 (3) (2016) 175–184.
[37] J. Coates, Interpretation of infrared spectra, a practical approach, Encycl. Anal. Chem. 18 (2000) 5606.
[38] J.V. Kadamne, C.L. Castrodale, A. Proctor, Measurement of conjugated linoleic acid (CLA) in CLA-rich potato chips by ATR-FTIR spectroscopy, J. Agric. Food Chem. 59 (6) (2011) 2190–2196.
[39] T.H. Ibrahim, Y. Chehade, M.A. Zour, Corrosion inhibition of mild steel using potato peel extract in 2 M HCL solution, Int. J. Electrochem. Sci. 6 (2011) 6542–6556.
[40] A. Pradeep, P. Priyadharsini, G. Chandrasekaran, Sol–gel route of synthesis of nanoparticles of $MgFe_2O_4$ and XRD, FTIR and VSM study, J. Magn. Magn. Mater. 320 (21) (2008) 2774–2779.
[41] N. Basavegowda, A. Sobczak-Kupiec, D. Malina, H.S. Yathirajan, V.R. Keerthi, N. Chandrashekar, S. Dinkar, P. Liny, Plant mediated synthesis of gold nanoparticles using fruit extracts of *Ananas comosus* (L.) (pineapple) and evaluation of biological activities, Adv. Mater. Lett. 4 (5) (2013) 332–337.
[42] V.S. Marangoni, I.M. Paino, V. Zucolotto, Synthesis and characterization of jacalin-gold nanoparticles conjugates as specific markers for cancer cells, Colloids Surf. B Biointerfaces 112 (2013) 380–386.
[43] R. Sanghi, P. Verma, pH dependant fungal proteins in the "green" synthesis of gold nanoparticles, Adv. Mater. Lett. 1 (3) (2010) 193–199.
[44] L. Li, J.Y. Chen, X. Wu, P.N. Wang, Q. Peng, Plasmonic gold nanorods can carry sulfonated aluminum phthalocyanine to improve photodynamic detection and therapy of cancers, J. Phys. Chem. B 114 (51) (2010) 17194–17200.
[45] O. Osifeko, T. Nyokong, Synthesis and physicochemical properties of zinc and indium phthalocyanines conjugated to quantum dots, gold and magnetic nanoparticles, Dyes Pigments 131 (2016) 186–200.
[46] O. Adegoke, E. Antunes, T. Nyokong, Nanoconjugates of CdTe@ZnS quantum dots with cobalt tetraamino-phthalocyanine: characterization and implications for the fluorescence recognition of superoxide anion, J. Photochem. Photobiol. Chem. 257 (2013) 11–19.
[47] R. Seoudi, G.S. El-Bahy, Z.A. El Sayed, FTIR, TGA and DC electrical conductivity studies of phthalocyanine and its complexes, J. Mol. Struct. 753 (1–3) (2005) 119–126.
[48] B. L'Azou, I. Passagne, S. Mounicou, M. Tréguer-Delapierre, I. Puljalté, J. Szpunar, R. Lobinski, C.C. Ohayon, Comparative cytotoxicity of cadmium forms ($CdCl_2$, CdO, CdS micro- and nanoparticles) in renal cells, Toxicol. Res. 3 (1) (2014) 32–41.
[49] S. Mukherjee, M. Dasari, S. Priyamvada, R. Kotcherlakota, V.S. Bollu, C.R. Patra, A green chemistry approach for the synthesis of gold nanoconjugates that induce the inhibition of cancer cell proliferation through induction of oxidative stress and their in vivo toxicity study, J. Mater. Chem. B 3 (18) (2015) 3820–3830.
[50] S. Sabella, A. Galeone, G. Vecchio, R. Cingolani, P.P. Pompa, Au NPs are toxic in vitro and in vivo: a review, J. Nanosci. Lett. 1 (3) (2011) 145–165.